Received: 16 August 2024 | Revised: 4 November 2024 | Accepted: 22 November 2024 | Published online: 27 November 2024

RESEARCH ARTICLE

Journal of Optics and Photonics Research
2025, Vol. 2(2) 104–110
DOI: 10.47852/bonviewJOPR42024116

BON VIEW PUBLISHING

Structural Model and Characteristics of a Nanopiezoactuator for Nanoresearch

S. M. Afonin[1,*]

[1]*National Research University of Electronic Technology, Russia*

Abstract: In this work, the structural model and characteristics of a nanopiezoactuator for nanoresearch were derived using the piezoelasticity equation and the differential equation of the nanopiezoactuator, applying methods from applied mathematical physics. A nanopiezoactuator is a piezomechanical device that converts electrical energy into mechanical energy, enabling the actuation of mechanisms and systems within the nanodisplacement range or controlling them via the inverse piezoelectric effect. A nanopiezoactuator is utilized for nanoalignment and nanopositioning, temperature and gravitational deformation compensation, and spatial movement in various fields, including nanoresearch, nanotechnology, microelectronics, nanobiotechnology, scanning microscopy, astronomy, adaptive optics, large compound telescopes, deformable mirrors, mechatronics, robotics, and medical microsurgical equipment. The schemes, functions, and characteristics of a nanopiezoactuator are obtained from its structural model by method of applied mathematical physics. The structural model of the transverse piezoactuator is obtained for the voltage control. The characteristics of the transverse piezoactuator are received. Piezoceramic from PbZr1-xTixO3 (PZT) lead zirconate titanate is widely used in a nanopiezoactuators for its reliability, high accuracy, and simple control. The characteristics of the PZT transverse actuator are determined.

Keywords: nanopiezoactuator, structural model and scheme, characteristic

1. Introduction

Method of applied mathematical physics is used. The characteristics of a nanopiezoactuator are received from piezoelasticity equation and differential equation. The static and characteristics of a nanopiezoactuator for nanoresearch are determined. The function of the transverse nanopiezoactuator is obtained. The characteristics of the PZT nanopiezoactuator are written. Its characteristics are used to describe the control systems for nanoresearch [1–15]. The PZT nanopiezoactuator is promising for nanotechnology, microscopy, nanoresearch, interferometry, adaptive optics, large compound telescope, and deformation mirror of telescope [16–28].

There are advantages of piezoceramics over other piezoelectrics, including a high piezoelectric effect, a high Curie point, stability of properties over time and across a wide temperature range, high mechanical strength, and relatively simple manufacturing technology that enables the production of piezoactuators in desired configurations. Piezoactuators are characterized by high accuracy, small overall dimensions, simple design and control, wide operating temperature range, high reliability, and cost effectiveness. The piezoeffect in piezoceramics appears after its polarization by a strong constant field. After its effect is complete, residual polarization remains, since domain reorientation processes have occurred. The most widely used piezoceramics are based on lead zirconate and titanate type PZT (PbZr1-xTixO3), which has high electromechanical activity [5, 16, 17]. The greatest interest in PZT is caused by its exceptional piezoproperties. Solid solutions of PbZr1-xTixO3 are characterized by the existence of a morphotropic phase boundary at the composition containing 53 mol.% PbZrO3. This is an almost vertical boundary on the phase diagram, separating the regions of the tetragonal and rhombohedral ferroelectric phases [5–25].

The core of this article focuses on nanopiezoactuators, which are integral to the fields of nanotechnology, mechatronics, materials science, optics, and photonics. The practical applications of nanopiezoactuators give nanometric characteristics for optical and optoelectronic systems. The transverse nanopiezoactuator cylindrical type with reinforcement is widely used in precision mechatronics systems in optics and nanoresearch, in medical equipment for precise instrument feed during microsurgical and eyesoperations, in laser technology, adaptive interferometers, electron microscopy with high precision and speed movement [6, 13].

The reinforced longitudinal nanopiezoactuator is the structure consisting of the piezoelectric packages reinforced with the pin or the spring with the beginning force. This longitudinal nanopiezoactuator provides precise positioning in different regimes before its opening structure when stretched. The reinforced longitudinal nanopiezoactuator is utilized for micro- and nano-displacements in fuel injection systems, precision metal cutting machines, magnetic section adjustments, adaptive optics, laser technology, and tunnel microscopy [6, 9].

The multilayer nanopiezoactuator consists of the films of the PZT piezomaterial with tens μm thickness and internal electrodes made from palladium and silver metals. This multilayer nanopiezoactuator is applied for the alignment of fiber optic systems, interferometers, adaptive optical systems, and stabilization systems [6, 11].

*Corresponding author: S. M. Afonin, National Research University of Electronic Technology, Russia. Emails: msf15@org.miet.ru, eduems@mail.ru

The bimorphic piezoactuator consists of two piezoelectric layers, where, during its bending operation, one piezoelectric layer is extended while the other is compressed. The displacement of the bimorphic piezoactuator is much greater than the displacement of the nanopiezoactuator with the correspondingly lower developed force and resonant frequency. The bimorphic piezoactuator is used for switching devices and scanning systems [1, 6, 11].

Let us consider the mechanism of torque generation for the vibrating piezoactuator using the example of a device with the piezoplate. When the piezoplate oscillates in two mutually perpendicular planes, depending on the amplitudes, frequencies, and phases of the disturbing forces, the end of the piezoelectric plate describes a trajectory of motion from a circle to an elongated ellipse. If an alternating voltage of a certain frequency is applied to the piezoplate, its linear size will periodically increase and decrease, and the piezoplate will perform longitudinal oscillations. As the voltage increases, the length of the piezoplate increases, and its end, together with the rotor, will move in the transverse direction. This is equivalent to the action of a transverse bending force, which causes transverse oscillations. When the end of the piezoplate comes into contact with the rotor of the piezoactuator, we obtain rotation of the rotor. The linear speed of rotation of the rotor depends on the amplitude and frequency of oscillations of the end of the piezoplate. The maximum amplitude of the piezoplate end face movement is limited by the strength limit of the material and by the overheating of the piezoplate. Overheating PZT piezoceramics above the critical temperature of the Curie point leads to the loss of piezoproperties. When the vibrating piezoactuator operates at the piezoplate temperature, an order of magnitude lower than the Curie point, the maximum power of the vibrating piezoactuator is limited by the strength limit of the piezoceramics [1–11].

Step piezoactuators have a range of movement of several tens of millimeters and an error of up to several nanometers [11]. The disadvantages of step piezoactuators are the low bandwidth of several hertz, the technological difficulties in obtaining stable supporting surfaces of clamps, the change in step due to wear of rubbing surfaces, and the design complexity.

For nanoresearch, a nanopiezoactuator is applied [1–9]. A nanopiezoactuator is used for alignment and positioning with nanometric error, compensation of temperature and gravitational deformations, spatial movement in nanoresearch, nanotechnology, microelectronics, nanobiotechnology, electron microscopy, astronomy, adaptive optics, mechatronics, and robotics. With the inverse piezoeffect, a linear change in the size of the piezoactuator occurs when the electric field changes. The structural general model, scheme, and functions of a nanopiezoactuator are obtained for nanoresearch.

2. Literature Review

A nanopiezoactuator in the form piezoplate is applied for nanoresearch, microelectronics, nanobiotechnology, scanning microscopy, astronomy, adaptive optics, compound telescope, deformation mirror, nanomedical tool for nanoposition, and nanocompensation deformations, This piezoplate is a piezomechanical device for transformations electrical energy in nanomechatronics systems to mechanical energy of the precision object with using inverse piezoeffect. Nanopiezoactuators are used in precision coordinate tables for nanopositioning objects along the X and Y axes. The solution of the linear ordinary differential equation is determined with boundary conditions of piezoplate and the equation of the inverse piezoeffect. The characteristics of a nanopiezoactuator for nanoresearch are received by method applied mathematical physics [10–28].

An increase in the range of movement to tens of micrometers is achieved through the use of the multilayer piezoactuator [1, 6, 11], the step piezoactuator, or the ultrasonic vibrating piezoactuator [12, 20]. Piezomaterials, including quartz, tourmaline, lithium sulfate, barium titanate [2], and ferroelectric ceramics [5–7, 9], based on lead zirconate and titanate type PZT (PbZr1-xTixO3), are widely used for the production of piezoactuators. The piezoeffect in ferroelectric ceramics appears after its polarization by a strong constant field [5–25].

Scanning tunneling microscope (STM) is used for educational purposes at the nanometer level. In its components and scanner are applied the piezoactuators. The nanomotion components and piezoscanner are controlled by using piezoactuators, then avoiding the thermal drift associated with engine control [26].

The fast positioning platform (FPP) is used on the high stiffness PZT piezoactuator and the flexible mechanism for precision machining. This fast positioning platform is driven by high stiffness PZT piezoactuator and guided by the flexible hinge-based mechanism. The flexible hinge mechanism provided planar motion capability with high stiffness and good guiding performance [27].

A nanopiezoactuator based on ferroelectric ceramics is characterized by high accuracy, small overall dimensions, simple design and control, wide operating temperature range, high reliability, and cost effectiveness. The static and dynamic characteristics of the PZT piezoactuator are determined as functions of the actuator's stiffness. The model of the nanopositioning system with the piezoactuators is obtained [15]. At present, XYZ micro- and nanopositioning systems with a piezoactuators on ferroelectric ceramics are used in micro- and nanomanipulations for nanoresearch [13, 15, 21–28].

3. Method

This article uses method of applied mathematical physics. The static and dynamic characteristics of a nanopiezoactuator for nanoresearch are received from a piezoelasticity and differential equation of a nanopiezoactuator. In general equation, piezoelasticity is determined [4–28]

$$S_i = \nu_{mi}\Psi_m + s_{ij}^{\Psi}T_j \tag{1}$$

here Ψ_m the control parameter is E_m the tension electric field at the voltage control or D_m the electric induction at the current control, ν_{mi} the piezoconstant is d_{mi} the piezomodule or g_{mi} the piezocoefficient, s_{ij}^{Ψ} the elastic compliance at $\Psi = \text{const}$, S_i is the relative displacement, T_j the tension mechanical field.

For nanoresearch, the differential equation [4, 8, 10] of a nanopiezoactuator is used

$$\frac{d^2\Xi(x,s)}{dx^2} - \gamma^2\Xi(x,s) = 0 \tag{2}$$

$$\gamma = s/c^E + \alpha$$

here $\Xi(x,s)$, s, x, γ, c^E, α are the Laplace transform of the nanodisplacement, the parameter, the coordinate and the propagation coefficient, the speed of sound at $E = \text{const}$, the attenuation coefficient.

The structural model of a nanopiezoactuator represents a system of Laplace transformation equations for the displacement of its ends due to the inverse piezoeffect (Equation (1)), which, accounting for the electromechanical parameters of the nanopiezoactuator, describes its structure and the conversion of electrical field energy into mechanical energy, the displacements, and forces corresponding to the ends of a nanopiezoactuator.

The problem of obtaining the structural model of a nanopiezoactuator for nano- and microdisplacement is solved using the method of applied mathematical physics. The solution

of the linear ordinary differential Equation (2) is found, taking into account the boundary conditions. The transfer functions of a nanopiezoactuator are determined from the structural model of a nanopiezoactuator for the nanomechatronic system.

The structural model of a nanopiezoactuator obtained in this work clearly reflects the transformation of electrical energy into mechanical energy, in contrast to the Mason's [5] electrical equivalent circuit of the piezotransducer. For the transverse piezoactuator, the equation of the inverse transverse piezoeffect is written [4–10]

$$S_1 = d_{31}E_3 + s_{11}^E T_1 \tag{3}$$

here S_1, d_{31}, E_3, s_{11}^E, T_1 are the relative deformation along axis 1, the transverse piezomodule, the electric field strength along axis 3, the elastic compliance along axis 1, and the mechanical stress along axis 1. In this inverse transverse piezoeffect equation $S_1 = S_i$, $d_{31} = \nu_{mi}$, $E_3 = \Psi_m$, $s_{11}^E = s_{ij}^\Psi$, $T_1 = T_j$.

The boundary conditions are defined

$$\Xi(0,s) = \Xi_1(s) \text{ at } x = 0 \tag{4}$$

$$\Xi(h,s) = \Xi_2(s) \text{at } x = h \tag{5}$$

The solution to the differential Equation (2) for the transverse deformation is written as

$$\Xi(x,s) = \frac{\Xi_1(s)\mathrm{sh}((h-x)\gamma) + \Xi_2(s))\mathrm{sh}(x\gamma)}{\mathrm{sh}(h\gamma)} \tag{6}$$

4. Structural Model

Let us consider the structural model of the transverse piezoactuator for the voltage control. The equations for the forces acting on the ends of the transverse piezoactuator are of the form

$$T_1(0,s)S_0 = F_1(s) + M_1 s^2 \Xi_1(s) \text{ at } x = 0 \tag{7}$$

$$T_1(h,s)S_0 = -F_2(s) - M_2 s^2 \Xi_2(s) \text{ at } x = h \tag{8}$$

The system of equations for mechanical stresses at the ends of the transverse piezoactuator for the voltage control at $x = 0$ and $x = h$ can be written as

$$T_1(0,s) = \frac{1}{s_{11}^E}\frac{d\Xi(x,s)}{dx}\bigg|_{x=0} - \frac{d_{31}}{s_{11}^E}E_3(s) \tag{9}$$

$$T_1(h,s) = \frac{1}{s_{11}^E}\frac{d\Xi(x,s)}{dx}\bigg|_{x=h} - \frac{d_{31}}{s_{11}^E}E_3(s) \tag{10}$$

From the inverse transverse piezoeffect (Equation (3)), the transform of the force is obtained

$$s_{11}^E F(s)/S_0 = d_{31}E_3(s) \tag{11}$$

From Equation (11), the transformation of force resulting in displacement due to the transverse piezoelectric effect is determined

$$F(s) = \frac{d_{31}S_0E_3(s)}{s_{11}^E} \tag{12}$$

From the Equation (12), the transverse reverse coefficient at the voltage control is obtained

$$k_r = \frac{F(s)}{U(s)} = \frac{d_{31}S_0}{\delta s_{11}^E} \tag{13}$$

This system of the equations for mechanical stresses (Equations (9) and (10)) gives the system of equations for the structural model of the transverse piezoactuator for the voltage control at the resistance $R = 0$. Then the structural model of the transverse piezoactuator for the voltage control has the form

$$\Xi_1(s) = (M_1 s^2)^{-1}\left\{\begin{array}{l} -F_1(s) + (\chi_{11}^E)^{-1}\times \\ \times\left[\begin{array}{l} d_{31}E_3(s) - [\gamma/\mathrm{sh}(h\gamma)] \\ \times[\mathrm{ch}(h\gamma)\Xi_1(s) - \Xi_2(s)] \end{array}\right] \end{array}\right\} \tag{14}$$

$$\Xi_2(s) = (M_2 s^2)^{-1}\left\{\begin{array}{l} -F_2(s) + (\chi_{11}^E)^{-1}\times \\ \times\left[\begin{array}{l} d_{31}E_3(s) - [\gamma/\mathrm{sh}(h\gamma)] \\ \times[\mathrm{ch}(h\gamma)\Xi_2(s) - \Xi_1(s)] \end{array}\right] \end{array}\right\} \tag{15}$$

$$\chi_{11}^E = s_{11}^E/S_0 \tag{16}$$

here M_1, M_2, $F_1(s)$, $F_2(s)$ are the masses of loads and the Laplace transforms of forces at the ends of the transverse piezoactuator.

From the equation of the inverse transverse piezoeffect (Equation (3)), the maximum transverse static nanodisplacement ξ_0 is obtained

$$\xi_0 = d_{31i}(h/\delta)U \tag{17}$$

where U is the voltage.

Electronic measuring system model 214 of Caliber plant was used for experimental observation of the static displacement for the piezoactuator. In the experiment for the PZT transverse piezoactuator at $d_{31} = 0.2$ nm/V, $h/\delta = 10$, $U = 300$ V its static displacement is received $\xi_0 = 600$ nm with 20% error.

From the structural model of the transverse piezoactuator (Equations (14)–(16)) for the voltage control, its transfer functions are determined

$$W_{11}(s) = \Xi_1(s)/E_3(s) = d_{31}[M_2\chi_{11}^E s^2 + \gamma\mathrm{th}(h\gamma/2)]/A_{11} \tag{18}$$

$$\begin{aligned} A_{11} = {} & M_1M_2(\chi_{11}^E)^2 s^4 + \{(M_1+M_2)\chi_{11}^E/[c^E\mathrm{th}(h\gamma)]\}s^3 + \\ & + \left[(M_1+M_2)\chi_{11}^E\alpha\Big/\mathrm{th}(h\gamma) + 1/(c^E)^2\right]s^2 + 2\alpha s/c^E + \alpha^2 \end{aligned} \tag{19}$$

$$W_{21}(s) = \Xi_2(s)/E_3(s) = d_{31}[M_1\chi_{11}^E s^2 + \gamma\mathrm{th}(h\gamma/2)]/A_{11} \tag{20}$$

$$W_{12}(s) = \Xi_1(s)/F_1(s) = -\chi_{11}^E[M_2\chi_{11}^E s^2 + \gamma/\mathrm{th}(h\gamma)]/A_{11} \tag{21}$$

$$\begin{aligned} W_{13}(s) &= \Xi_1(s)/F_2(s) = \\ &= W_{22}(s) = \Xi_2(s)/F_1(s) = [\chi_{11}^E\gamma/\mathrm{sh}(h\gamma)]/A_{11} \end{aligned} \tag{22}$$

$$W_{23}(s) = \Xi_2(s)/F_2(s) = -\chi_{11}^E[M_1\chi_{11}^E s^2 + \gamma/\mathrm{th}(h\gamma)]/A_{11} \tag{23}$$

Then, for the transverse piezoactuator for the voltage control at $R = 0$, $\alpha = 0$, $M_1 = 0$, $M_2 = 0$ the expression for mechanical resonance has the form

$$\mathrm{tg}(kh/2) = \infty \tag{24}$$

here $k = \omega/c^E$ is frequency coefficient; ω is circular frequency.

This is because

$$k_i h = \pi(2i-1) \tag{25}$$

where index $i = 1, 2, 3, \ldots$.

Therefore, for the Equation (25) the transverse piezoactuator is the half-wave vibrator with resonance frequency

$$f_1 = c^E/(2h) \tag{26}$$

Microscope MIN-8 was used for experimental observation of the resonance for the piezoactuator. In the experiment for the PZT transverse actuator at $c^E = 3{\cdot}10^3$ m/s and $h = 2.5{\cdot}10^{-2}$ m, its mechanical resonance frequency is obtained as $f_1 = 60$ kHz with 20% error.

5. Structural Scheme

The structural general model, scheme and functions a nanopiezoactuator are obtained for nanoresearch by method of applied mathematical physics.

In general at $x = 0$ and $x = l$ for $l = \{\delta, h, b$, the system of the boundary conditions [4, 8, 10] for a nanopiezoactuator is obtained

$$T_j(0,s) = \frac{1}{s_{ij}^{\Psi}} \frac{d\Xi(x,s)}{dx}\bigg|_{x=0} - \frac{\nu_{mi}}{s_{ij}^{\Psi}} \Psi_m(s) \tag{27}$$

$$T_j(l,s) = \frac{1}{s_{ij}^{\Psi}} \frac{d\Xi(x,s)}{dx}\bigg|_{x=l} - \frac{\nu_{mi}}{s_{ij}^{\Psi}} \Psi_m(s) \tag{28}$$

From the equation piezoelasticity, the transform of the force is obtained

$$s_{ij}^{\Psi} F(s)/S_0 = \nu_{mi} \Psi_m(s) \tag{29}$$

Then from the Equation (29), the transform of the force causes displacement is determined

$$F(s) = \frac{\nu_{mi} S_0 \Psi_m(s)}{s_{ij}^{\Psi}} \tag{30}$$

The reverse coefficient at the voltage control with $U(s) = E_m(s)\delta$ from the Equation (30) is determined in the form

$$k_r = \frac{F(s)}{U(s)} = \frac{d_{mi} S_0}{\delta s_{ij}^E} \tag{31}$$

The structural general model and scheme a nanopiezoactuator from the mechanical stresses (Equations (27) and (28)) are obtained on Figure 1

$$\Xi_1(s) = (M_1 s^2)^{-1} \left\{ \begin{array}{l} -F_1(s) + \left(\chi_{ij}^{\Psi}\right)^{-1} \times \\ \times \left[\begin{array}{l} \nu_{mi} \Psi_m(s) - [\gamma/\mathrm{sh}(l\gamma)] \\ \times [\mathrm{ch}(l\gamma)\Xi_1(s) - \Xi_2(s)] \end{array} \right] \end{array} \right\} \tag{32}$$

$$\Xi_2(s) = (M_2 s^2)^{-1} \left\{ \begin{array}{l} -F_2(s) + \left(\chi_{ij}^{\Psi}\right)^{-1} \times \\ \times \left[\begin{array}{l} \nu_{mi} \Psi_m(s) - [\gamma/\mathrm{sh}(l\gamma)] \\ \times [\mathrm{ch}(l\gamma)\Xi_2(s) - \Xi_1(s)] \end{array} \right] \end{array} \right\} \tag{33}$$

$$\chi_{ij}^{\Psi} = s_{ij}^{\Psi} \Big/ S_0 \tag{34}$$

Figure 1
General scheme nanopiezoactuator

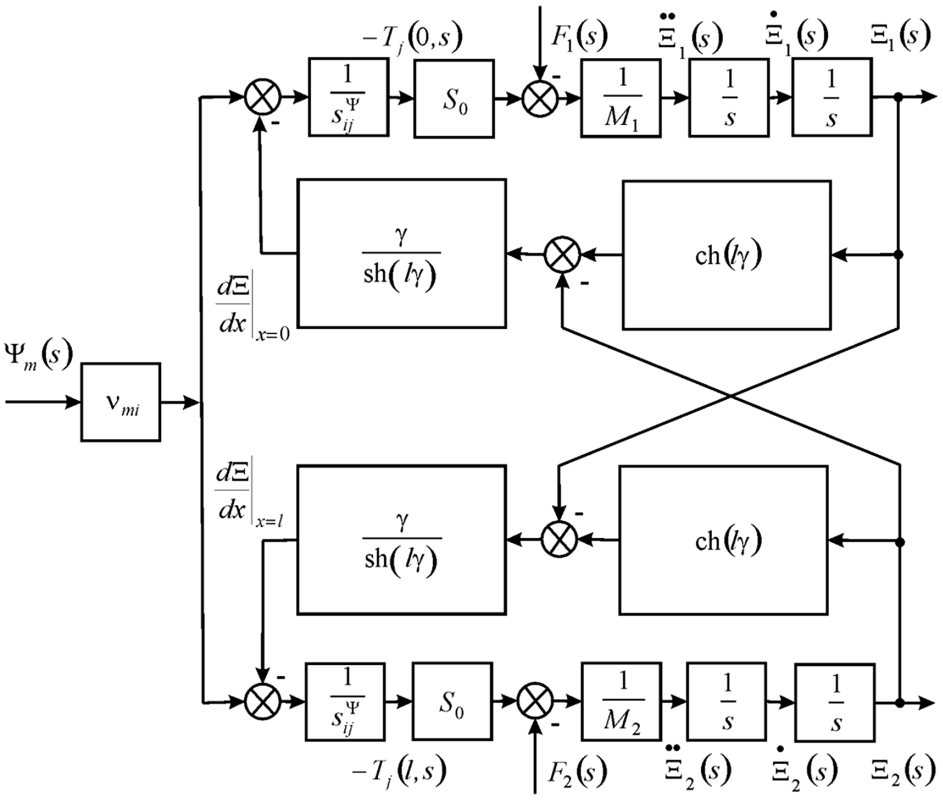

Here

$$\nu_{mi} = \begin{Bmatrix} d_{33}, d_{31}, d_{15} \\ g_{33}, g_{31}, g_{15} \end{Bmatrix}, \ \Psi_m = \begin{Bmatrix} E_3, E_3, E_1 \\ D_3, D_3, D_1 \end{Bmatrix} \tag{35}$$

$$s_{ij}^{\Psi} = \begin{Bmatrix} s_{33}^{E}, s_{11}^{E}, s_{55}^{E} \\ s_{33}^{D}, s_{11}^{D}, s_{55}^{D} \end{Bmatrix}, \ \gamma = \{\gamma^{E}, \ \gamma^{D}, \ c^{\Psi} = \{ \ c^{E}, \ c^{D} \tag{36}$$

The general model and scheme of a nanopiezoactuator in Figure 1 are used to calculate systems for nanoresearch.

From the Equations (32)–(34), the matrix equation of the nanodisplacements is determined

$$\begin{pmatrix} \Xi_1(s) \\ \Xi_2(s) \end{pmatrix} = \begin{pmatrix} W_{11}(s) & W_{12}(s) & W_{13}(s) \\ W_{21}(s) & W_{22}(s) & W_{23}(s) \end{pmatrix} \begin{pmatrix} \Psi_m(s) \\ F_1(s) \\ F_2(s) \end{pmatrix} \tag{37}$$

here its functions

$$W_{11}(s) = \Xi_1(s)/\Psi_m(s) = \nu_{mi}\left[M_2\chi_{ij}^{\Psi}s^2 + \gamma\text{th}(l\gamma/2)\right]\Big/A_{ij} \tag{38}$$

$$A_{ij} = M_1M_2\left(\chi_{ij}^{\Psi}\right)^2 s^4 + \left\{(M_1 + M_2)\chi_{ij}^{\Psi}\Big/[c^{\Psi}\text{th}(l\gamma)]\right\}s^3 + \\ + \left[(M_1 + M_2)\chi_{ij}^{\Psi}\alpha\Big/\text{th}(l\gamma) + 1/(c^{\Psi})^2\right]s^2 + 2\alpha s/c^{\Psi} + \alpha^2 \tag{39}$$

$$W_{21}(s) = \Xi_2(s)/\Psi_m(s) = \nu_{mi}\left[M_1\chi_{ij}^{\Psi}s^2 + \gamma\text{th}(l\gamma/2)\right]\Big/A_{ij} \tag{40}$$

$$W_{12}(s) = \Xi_1(s)/F_1(s) = -\chi_{ij}^{\Psi}\left[M_2\chi_{ij}^{\Psi}s^2 + \gamma/\text{th}(l\gamma)\right]\Big/A_{ij} \tag{41}$$

$$W_{13}(s) = \Xi_1(s)/F_2(s) = \\ = W_{22}(s) = \Xi_2(s)/F_1(s) = \left[\chi_{ij}^{\Psi}\gamma\Big/\text{sh}(l\gamma)\right]\Big/A_{ij} \tag{42}$$

$$W_{23}(s) = \Xi_2(s)/F_2(s) = -\chi_{ij}^{\Psi}\left[M_1\chi_{ij}^{\Psi}s^2 + \gamma/\text{th}(l\gamma)\right]\Big/A_{ij} \tag{43}$$

Let us consider the structural model and scheme of the transverse piezoactuator for the voltage control at $R \neq 0$ on Figure 2.

To calculate the back electromotive force of the transverse piezoactuator [4, 5, 8, 10], the equation of the direct transverse piezoeffect is used

$$D_3 = d_{31}T_1 + \varepsilon_{33}^{T}E_3 \tag{44}$$

where D_3, ε_{33}^{T} are the electric induction along axis 3 and the permittivity.

The direct coefficient k_d for the transverse piezoactuator is written

$$k_d = \frac{d_{31}S_0}{\delta s_{11}^{E}} \tag{45}$$

From the Equation (45), the transform of the voltage for the back electromotive force of transverse piezoactuator on Figure 2 is determined

$$U_d(s) = \frac{d_{31}S_0R}{\delta s_{11}^{E}}\dot{\Xi}_n(s) = k_dR\dot{\Xi}_n(s) \tag{46}$$

$$n = 1, \ 2$$

where n is the number end.

Then the transverse static nanodisplacements for the transverse piezoactuator at the voltage control are determined from the Equations (18) and (20) by the expressions

$$\xi_1 = d_{31}(h/\delta)UM_2/(M_1 + M_2) \tag{47}$$

Figure 2
Scheme transverse piezoactuator with back electromotive force

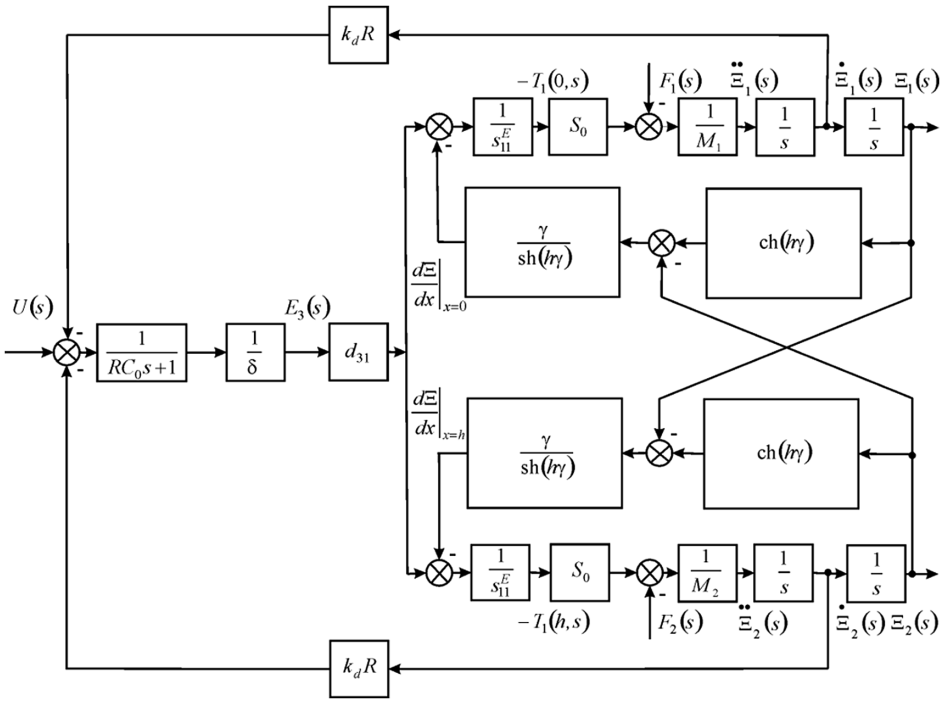

$$\xi_2 = d_{31}(h/\delta)UM_1/(M_1 + M_2) \tag{48}$$

In the experiment for the PZT transverse piezoactuator at $d_{31} = 0.2$ nm/V, $h/\delta = 10$, $U = 300$ V, $M_1 = 0.25$ kg, $M_2 = 1$ kg its static displacements are obtained $\xi_1 = 480$ nm, $\xi_2 = 120$ nm with 20% error.

For a fixed first end of the transverse nanopiezoactuator, the boundary conditions are expressed in the following form

$$\Xi(0, s) = 0 \text{ for } x = 0 \tag{49}$$

$$\Xi(h, s) = \Xi_2(s) \text{ for } x = h \tag{50}$$

then the solution of the differential Equation (2) at fixed first end of the transverse nanopiezoactuator

$$\Xi(x, s) = \frac{\Xi_2(s)\ \mathrm{sh}(x\gamma)}{\mathrm{sh}(h\gamma)} \tag{51}$$

From the Equations (2), (10) and (51), the expression for the transverse nanopiezoactuator has the form

$$\frac{\Xi_2(s)\gamma}{\mathrm{th}(h\gamma)} + \frac{\Xi_2(s)s_{11}^E M_2 s^2}{S_0} + \frac{\Xi_2(s)s_{11}^E C_l}{S_0} = d_{31}E_3(s) \tag{52}$$

Then its function for $R = 0$ from the Equation (52) is determined

$$W(s) = \frac{\Xi_2(s)}{U(s)} = \frac{d_{31}(h/\delta)}{M_2 p^2/C_{11}^E + h\gamma\mathrm{cth}(h\gamma) + C_e/C_{11}^E} \tag{53}$$

where $\Xi_2(s)$, C_{11}^E, C_e are the transform nanodisplacement of its end, the stiffness actuator, and load.

For elastic-inertial load $M_2 >> m$ from the Equation (53), the function is received

$$W(s) = \frac{\Xi(s)}{U(s)} = \frac{k_{31}^U}{T_t^2 s^2 + 2T_t\xi_t s + 1} \tag{54}$$

$$k_{31}^U = d_{31}(h/\delta)/(1 + C_e/C_{11}^E),\ T_t = \sqrt{M_2/(C_e + C_{11}^E)} \tag{55}$$

$$\omega_t = 1/T_t \tag{56}$$

For experimental observation of the resonance, Microscope MIN-8 was used. In the experiment for the PZT actuator $C_e = 0.33{\cdot}10^7$ N/m, $C_{11}^E = 3{\cdot}10^7$ N/m, $M_2 = 1$ kg, its parameter in dynamic is obtained $\omega_t = 5.8{\cdot}10^3$ s^{-1} with 20% error.

The static nanodisplacement from the Equation (55) is obtained

$$\Delta h = \frac{d_{31}(h/\delta)U}{1 + C_e/C_{11}^E} = k_{31}^U U \tag{57}$$

In the experiment for the PZT transverse piezoactuator at $d_{31} = 0.2$ nm/V, $h/\delta = 10$, $U = 300$ V, $C_e/C_{11}^E = 0.1$, its transform coefficient and static displacement are determined $k_{31}^U = 1.8$ nm/V, $\Delta h = 540$ nm with 20% error.

Its mechanical characteristic from the Equation (3) has the form

$$\Delta h = \Delta h_{\max}(1 - F/F_{\max}) \tag{58}$$

$$\Delta h_{\max} = d_{31}(h/\delta)U,\ F_{\max} = d_{31}S_0E_3/s_{11}^E \tag{59}$$

In the experiment for the PZT transverse piezoactuator at $h/\delta = 10$, $U = 300$ V, $E_3 = 3{\cdot}10^5$ V/m, $S_0 = 2{\cdot}10^{-5}$ m^2, $d_{31} = 0.2$ nm/V, $s_{11}^E = 10{\cdot}10^{-12}$ m^2/N its maximum static displacement and force are obtained $\Delta h_{\max} = 600$ nm, $F_{\max} = 120$ N on Figure 3 with 20% error.

Figure 3
Transverse mechanical characteristic

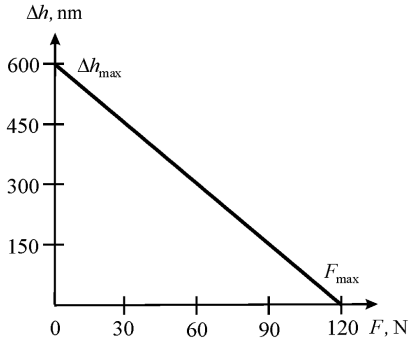

In the article, the characteristics of the PZT nanoactuator are received. The PZT nanoactuator is promising for nanoresearch.

6. Discussion

Piezoactuators are characterized by high accuracy, small overall dimensions, simple design and control, wide operating temperature range, high reliability, and cost effectiveness. The nanopiezoactuators from ferroelectric ceramics, based on lead zirconate and titanate type PZT, are promising for nanoresearch. The PZT nanopiezoactuator is used for nanodisplacement in nanoresearch and nanotechnology.

The characteristics of a nanopiezoactuator are received from piezoelasticity equation and differential equation by using method of applied mathematical physics. The static and dynamic characteristics of the nanopiezoactuator are determined. The PZT transverse actuator is widely used for nanoresearch, interferometers, adaptive optics, medical equipment for precise instrument feed during microsurgical eyesoperations. The parameters of the nanopiezoactuator are obtained for nanoresearch.

7. Conclusion

The micro- and nanopositioning systems for precision displacements with a piezoactuators are used in nanomanipulations for nanoresearch. The structural general model, scheme, and functions of a nanopiezoactuator are received by using method of applied mathematical physics from the piezoelasticity equation and the differential equation of a nanopiezoactuator. The parameters of the characteristics PZT actuator are determined. The transverse PZT nanopiezoactuator with reinforcement is widely used in precision mechatronics systems in optics and nanoresearch, laser technology and optics for adaptive interferometer, large compound telescope, and deformation mirror of telescope. The functions of the transverse nanopiezoactuator are obtained for nanoresearch.

Ethical Statement

This study does not contain any studies with human or animal subjects performed by the author.

Conflicts of Interest

The author declares that he has no conflicts of interest to this work.

Data Availability Statement

Data sharing is not applicable to this article as no new data were created or analyzed in this study.

Author Contribution Statement

S. M. Afonin: Conceptualization, Methodology, Software, Validation, Formal analysis, Investigation, Resources, Data curation, Writing – original draft, Writing – review & editing, Visualization, Supervision, Project administration.

References

[1] Uchino, K. (1997). *Piezoelectric actuators and ultrasonic motors*. USA: Springer.

[2] Gao, J., Xue, D., Liu, W., Zhou, C., & Ren, X. (2017). Recent progress on $BaTiO_3$-based piezoelectric ceramics for actuator applications. *Actuators*, *6*(3), 24. https://doi.org/10.3390/act6030024

[3] Shevtsov, S. N., Soloviev, A. N., Parinov, I. A., Cherpakov, A. V., & Chebanenko, V. A. (2018). *Piezoelectric actuators and generators for energy harvesting: Research and development*. Switzerland: Springer. https://doi.org/10.1007/978-3-319-75629-5

[4] Afonin, S. M. (2008). Structural parametric model of a piezoelectric nanodisplacement transducer. *Doklady Physics*, *53*(3), 137–143. https://doi.org/10.1134/S1028335808030063

[5] Mason, W. P. (1965). Physical acoustics, principles and methods. *Physics Today*, *18*(12), 67. https://doi.org/10.1063/1.3047043

[6] Liu, Y., Zeng, A., Zhang, S., Ma, R., & Du, Z. (2022). An experimental investigation on polarization process of a PZT-52 tube actuator with interdigitated electrodes. *Micromachines*, *13*(10), 1760. https://doi.org/10.3390/mi13101760

[7] Parinov, I. A. (2015). *Piezoelectrics and nanomaterials: Fundamentals, developments and applications*. USA: Nova Science Publishers.

[8] Afonin, S. M. (2018). Structural-parametric model of electromagnetoelastic actuator for nanomechanics. *Actuators*, *7*(1), 6. https://doi.org/10.3390/act7010006

[9] Chen, C., Shi, Y., Zhang, J., & Wang, J. (2016). Novel linear piezoelectric motor for precision position stage. *Chinese Journal of Mechanical Engineering*, *29*(2), 378–385. https://doi.org/10.3901/CJME.2015.1216.149

[10] Afonin, S. M. (2024). Structural scheme of an electromagnetoelastic actuator for nanotechnology research. In *Physics and Mechanics of New Materials and Their Applications: Proceedings of the International Conference*, 486–501. https://doi.org/10.1007/978-3-031-52239-0_45

[11] Spanner, K., & Koc, B. (2016). Piezoelectric motors, an overview. *Actuators*, *5*(1), 6. https://doi.org/10.3390/act5010006

[12] Zhao, C. (2011). *Ultrasonic motors: Technologies and applications*. Germany: Springer. https://doi.org/10.1007/978-3-642-15305-1

[13] Belfiore, N. P. (2018). Micromanipulation: A challenge for actuation. *Actuators*, *7*(4), 85. https://doi.org/10.3390/act7040085

[14] Toledo, J., Ruiz-Díez, V., Hernando-García, J., & Sánchez-Rojas, J. L. (2020). Piezoelectric actuators for tactile and elasticity sensing. *Actuators*, *9*(1), 21. https://doi.org/10.3390/act9010021

[15] Ferrara-Bello, A., Vargas-Chable, P., Vera-Dimas, G., Vargas-Bernal, R., & Tecpoyotl-Torres, M. (2021). XYZ micropositioning system based on compliance mechanisms fabricated by additive manufacturing. *Actuators*, *10*(4), 68. https://doi.org/10.3390/act10040068

[16] Limpichaipanit, A., & Ngamjarurojana, A. (2023). Strain characteristics of PLZT-based ceramics for actuator applications. *Actuators*, *12*(2), 74. https://doi.org/10.3390/act12020074

[17] Koc, B., Kist, S., & Hamada, A. (2023). Wireless piezoelectric motor drive. *Actuators*, *12*(4), 136. https://doi.org/10.3390/act12040136

[18] Zhao, C., Li, Z., Xu, F., Zhang, H., Sun, F., Jin, J., . . . , & Yang, L. (2024). Design of a novel three-degree-of-freedom piezoelectric-driven micro-positioning platform with compact structure. *Actuators*, *13*(7), 248. https://doi.org/10.3390/act13070248

[19] Yan, L., Jiang, A., Jiang, F., Liu, G., Wang, F., & Wu, X. (2022). Design and performance analysis of a micro-displacement worktable based on flexure hinges. *Micromachines*, *13*(4), 518. https://doi.org/10.3390/mi13040518

[20] Huang, L., Wang, Y., Cheng, F., Yu, Q., & Huang, W. (2024). Piezoelectric linear motors with alternating action for motion servo system of probe station. *Actuators*, *13*(8), 288. https://doi.org/10.3390/act13080288

[21] Cui, F., Li, Y., & Qian, J. (2021). Development of a 3-DOF flexible micro-motion platform based on a new compound lever amplification mechanism. *Micromachines*, *12*(6), 686. https://doi.org/10.3390/mi12060686

[22] Huang, W., Lian, J., Chen, M., & An, D. (2021). Bidirectional active piezoelectric actuator based on optimized bridge-type amplifier. *Micromachines*, *12*(9), 1013. https://doi.org/10.3390/mi12091013

[23] Ma, X., Liu, Y., Deng, J., Zhang, S., & Liu, J. (2022). A walker-pusher inchworm actuator driven by two piezoelectric stacks. *Mechanical Systems and Signal Processing*, *169*, 108636. https://doi.org/10.1016/j.ymssp.2021.108636

[24] Bhushan, B. (2017). *Springer handbook of nanotechnology*. Germany: Springer. https://doi.org/10.1007/978-3-662-54357-3

[25] Nalwa, H. S. (2019). *Encyclopedia of nanoscience and nanotechnology*. USA: American Scientific Publishers.

[26] Ma, W. (2024). Open STM: A low-cost scanning tunneling microscope with a fast approach method. *HardwareX*, *17*, e00504. https://doi.org/10.1016/j.ohx.2023.e00504

[27] Hu, G., Xin, W., Zhang, M., Chen, G., Man, J., & Tian, Y. (2024). Development of a fast positioning platform with a large stroke based on a piezoelectric actuator for precision machining. *Micromachines*, *15*(8), 1050. https://doi.org/10.3390/mi15081050

[28] Patel, J. K., & Pathak, Y. V. (2021). *Emerging technologies for nanoparticle manufacturing*. Switzerland: Springer. https://doi.org/10.1007/978-3-030-50703-9

How to Cite: Afonin, S. M. (2025). Structural Model and Characteristics of a Nanopiezoactuator for Nanoresearch. *Journal of Optics and Photonics Research*, *2*(2), 104–110. https://doi.org/10.47852/bonviewJOPR42024116